**Title**
INTERFEROMETRIC STUDY OF TRANSIENT DIFFUSION LAYERS



**Authors**
McLarnon, F.R.
Muller, R.H.
Tobias, C.W.

**Publication Date**
1975-06-01

Submitted to Electrochimica Acta

LBL-3550
Preprint

# INTERFEROMETRIC STUDY OF TRANSIENT DIFFUSION LAYERS

F. R. McLarnon, R. H. Muller, and C. W. Tobias

June 1975

Prepared for the U.S. Energy Research and Development Administration under Contract W-7405-ENG-48



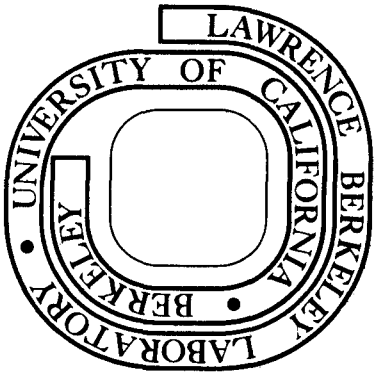

## DISCLAIMER

LBL-3550

# INTERFEROMETRIC STUDY OF TRANSIENT DIFFUSION LAYERS

F. R. McLarnon, R. H. Muller and C. W. Tobias

Inorganic Materials Research Division, Lawrence Berkeley Laboratory and
Department of Chemical Engineering; University of California
Berkeley, California 94720

## ABSTRACT

Transient refractive-index fields in stagnant $CuSO_4$ solutions were measured by double beam interferometry during the galvanostatic deposition of copper. Concentration profiles in the electrolyte have been derived from the interferograms by correcting for optical aberrations caused by beam deflection and reflection. The time-dependent concentration profiles are in good agreement with those derived from a solution of the diffusion equation in which the concentration dependence of diffusivity is taken into account.

Key Words: Interferometry; Transient diffusion; variable transport properties; Mass transfer; Electrodeposition

Concentration changes in the electrolyte near working electrodes result from transport processes in electrochemical processes.[1] We have used double-beam interferometry[2] for the investigation of concentration fields near electrodes. This technique offers the advantages of continuous observation with high resolution of concentration ($\sim 10^{-5}$ M) and distance ($\sim 10^{-4}$ cm) without disturbing transport or electrode processes, and is not restricted to limiting current density. Interferometry in its present form is, however, suitable only for the determination of concentration profiles in binary systems, i.e., when the local refractive-index is determined by the concentration of a single solute. For this reason, the method is as yet not applicable when a supporting electrolyte (e.g., $H_2SO_4$ in the case of copper deposition) is present.

Previous interferometric studies[3-6] of concentration changes in electrochemical systems have been based on the conventional interpretation[2] of interferograms, in which local phase change in the interferogram is simply related to local refractive-index (i.e., concentration) variation in the object. Such interpretation assumes that all light rays travel along straight paths as they traverse the specimen. We have shown, however, that deflection (refraction, Schlieren effect) of the beam, as it passes through the refractive-index field, from a straight path can lead to large errors.[7,8] We have also found that reflection[9] of light rays from the even slightly rounded edge of an otherwise planar electrode surface can likewise lead to significant errors in interpretation. These optical distortions must, therefore, be taken into account if reliable

information regarding interfacial concentration, concentration gradient and boundary layer thickness is to be obtained from experimental interferograms.

It is the purpose of this paper to compare concentration profiles, derived from the interferometric observation of diffusion layers by the use of procedures[8,9] which account for light deflection- and reflection, with those predicted on theoretical grounds.

## EXPERIMENTAL

A cross-sectional schematic of the interferometer and electrochemical cell is presented in Fig. 1. The 1×3.8 cm copper electrode blocks A and C were separated by the distance h = 2.5 cm. The electrolyte temperature was 20°C ± 1°C.

The side of each electrode facing the light beam was polished flat (within 0.03° from tangent plane) and smooth (0.3 μm peak-to-peak) using progressively finer (to #200) carbide paper, chromium oxide and diamond paste (1.0 μm) abrasives with kerosene as a lubricant. Each electrode working surface was then polished in a similar manner using a right-angle polishing jig that was kept in non-abrasive contact with the previously polished side in order to abrade the working surface at right angle to the side. The resulting electrode working surface was flat to within 1.0 μm over 80% of its width and showed a 1.0 μm peak-to-peak roughness. This procedure caused the electrode working surfaces to be

slightly rounded such that the edges were 0.01 mm lower than the center of the surface. The surface profiles were measured with a stylus surface analyzer[10] and are shown elsewhere.[9,11]

This electrode preparation permitted alignment of the test beam to be parallel to the electrode working surface within 0.1° by reflecting the beam from the polished side of the electrode such that it retraced its path to the source. The effect of beam misalignment on the fringe pattern has been discussed by Beach et al.[7]

The traveling dual-emission laser interferometer was mounted on a lathe bed to permit scanning of the concentration field along the length of the electrodes. (Details of the interferometer and the electrochemical cell have been given elsewhere.[12,13].) The cathode was observed in two horizontal orientations, facing up and facing down. Constant current of 5.0 and 10.0 $mA/cm^2$ was passed through the cell. The interferograms of the resulting transient diffusion layers were recorded by a Bolex Paillard 16 mm motion picture camera on Kodak Plus-X film at 20 frames/sec. The camera was positioned such that the plane of focus (optically conjugate to the camera film plane) was located on the inside of the glass wall farthest from the camera, where scale lines of 0.5 mm separation had been etched in the glass. We have previously justified the use of this plane of focus[7] for the interferometric observation of cathodic boundary layers. The experimental phase vs distance information was read from the interferograms by tracing fringes in a projection of the film onto a table with about 200-fold magnification.

## THEORY OF TRANSPORT

The convection-free electrodeposition of a metal cation from a stagnant aqueous binary salt electrolyte is described by the unsteady diffusion equation in one dimension:

$$\frac{\partial C}{\partial t} = \frac{\partial}{\partial x}\left(D \frac{\partial C}{\partial x}\right) \tag{1}$$

Equation (1) accounts for variation of the diffusion coefficient D with electrolyte concentration C. It represents a simplification* of the complete diffusion equation (see for example page 225 of Ref. 1). Current density is related to the interfacial concentration gradient by:

$$i = \frac{zFD}{1 - t_+} \left.\frac{\partial C}{\partial x}\right|_{x=0} \tag{2}$$

For galvanostatic electrodeposition, the boundary conditions to Eq. (1) are:

$$\frac{\partial C}{\partial x} = \frac{i(1 - t_+)}{zFD} \quad \text{at} \quad x = 0 \ , \ t > 0 \tag{3}$$

$$C = C_b \quad \text{at} \quad t \leqslant 0 \ , \ \text{all } x \tag{4}$$

$$C = C_b \quad \text{as} \quad x \to \infty \ , \ \text{all } t \tag{5}$$

If the diffusion coefficient D and cation transference number $t_+$ are assumed invarient with concentration, the solution of Eq. (1) with the boundary conditions (3) to (5) is the well-known Sand equation.[8,18]

---

*Variations of the cation transference number $t_+$ are not accounted for in Eq. (1).

The variation of the $CuSO_4$ diffusion coefficient over the range 0-0.1 M $CuSO_4$ is illustrated in Fig. 2. Smoothed data of Eversole, Kindsvater and Peterson,[16] corrected to 20°C, are indicated by the solid curve. We can approximate the physical property variations as linear functions of electrolyte concentration:

$$\frac{D}{D_o} = 1 - \alpha\theta \tag{6}$$

$$\frac{1 - t_+}{(1 - t_+)_o} = 1 + \gamma\theta \tag{7}$$

The subscripted properties correspond to zero electrolyte concentration, and $\theta$ is a dimensionless concentration $C/C_b$. Two linear approximations are shown on Fig. 2, each indicating the proper value of diffusion coefficient at C = 0.1 M $CuSO_4$. The curve for $\alpha = 0.0869$ accurately represents the data for $0.04\ M \leq C \leq 0.10\ M$, while the curve for $\alpha = 0.141$ approximates the data over the entire range $0 \leq C \leq 0.1$ M. The variation of cupric ion transference number measured by Fritz and Fuget[17] can be represented by $(1 - t_+)_o = 0.597$ and $\gamma = 0.0648$ ($t_+ = 0.403 - 0.387C$) over the range $0 \leq C \leq 0.1$ M $CuSO_4$.

The appropriate equations of unsteady diffusion can now be derived (using Eqs. (1) through (7)):

$$\frac{\partial\theta}{\partial t} = D_o\left[(1 - \alpha\theta)\,\frac{\partial^2\theta}{\partial x^2} - \alpha\left(\frac{\partial\theta}{\partial x}\right)^2\right] \tag{8}$$

$$\theta = 1 \quad \text{at} \quad t \leq 0 \quad , \quad \text{all } x \tag{9}$$

$$\theta = 1 \quad \text{as} \quad x \to \infty \tag{10}$$

$$\frac{\partial\theta}{\partial x} = \frac{i(1 - t_+)_o}{z F D_o C_b} \frac{1 + \gamma\theta}{1 - \alpha\theta} \quad \text{at} \quad x = 0 \, , \; t > 0 \tag{11}$$

These equations can be solved by standard numerical techniques. Casting the equations into Crank-Nicholson finite difference representation[14] and solving the resulting system of nonlinear algebraic equations by the Thomas method[15] determines the theoretical concentration profiles to within about 0.0002 M $CuSO_4$.

Concentration profiles were calculated from Eqs. (8) through (11) using the above-mentioned numerical techniques. For $\alpha = \gamma = 0$, the numerical solution matches the closed-form solution (Sand equation[8,18]) to within 0.0002 M $CuSO_4$ for step sizes of 0.001 mm and 0.1 sec.

## INTERPRETATION OF INTERFEROGRAMS

Figure 3 illustrates the analysis of a single interferogram recorded at a downward facing cathode after 30 sec of electrolysis at 10.0 $mA/cm^2$. The ordinate denotes distance from the true image of the electrode surface (undistorted by refraction or reflection). The abscissa relates electrolyte concentration to interferometric phase change (number of fringes) according to the conventional interpretation of interferograms. The location of the true interface $x = 0$ on the experimental interferogram has been determined by the method of focal plane variation outlined in Ref. 9. This technique locates the interface to within about 0.01 mm when no refractive-index gradients are present in the electrolyte (i.e., before beginning the electrolysis). With the interface $x = 0$ thus defined, the phase vs distance information obtained from analysis of the film can be plotted as the experimental interferogram depicted by the open circles on Fig. 3.

The experimental interferogram is now interpreted by a method[19] that accounts for light-deflection in the refractive-index field. This iterative technique determines the concentration profile (dashed line in Fig. 3) associated with a computed interferogram (solid line in Fig. 3) that best matches the experimental interferogram. The good agreement can be seen by comparing the computed and experimental interferograms in Fig. 3.

At this juncture, the shape of the computed interferogram may well agree with the shape of the experimental interferogram. However, the computed fringe could suggest, on the interferogram, an apparent interfacial location B different from A, indicated by the experimental interferogram (neither of which corresponds to the true interfacial location $x = 0$). Small (0.01 mm) errors in the original determination of the true interfacial location can have a comparable (0.02 mm) effect on this difference between experimental (A) and computed (B) end points.

Reflection from the edge of the electrode surface when refractive-index gradients are present in the electrolyte can have an effect much like reflection when no gradients are present: the apparent interfacial location can be different from the location expected considering light-deflection alone. Reflection thus causes two source of error: (a) an 0.01 mm uncertainty in the determination of the true interfacial location without refractive-index gradients present in the electrolyte and (b) 0.02 mm uncertainty in measurement of the apparent interfacial location when refractive-index gradients are present.

## RESULTS

The interferometrically derived transient interfacial concentrations for an experiment at 10 $mA/cm^2$ are shown in Fig. 4. Also shown are the theoretical interfacial concentrations for $\alpha = 0$ (Sand equation) and for $\alpha = 0.0869$ and $\alpha = 0.141$. While the uncertainty in derived interfacial concentrations precludes assigning a particular value of $\alpha$ as best representing the variation of diffusion coefficient with concentration, the results do suggest better experimental agreement with numerical solutions for variable physical properties than with the Sand equation. The cell voltage is also plotted, illustrating the rapid rise in electrode potential as limiting transport conditions are approached. Our interpretation of interferograms, contrary to conventional interpretation, shows that the interfacial concentration, indeed, becomes vanishingly small as limiting current conditions are reached.

Figure 5 compares the interferometrically derived transient interfacial concentrations for two different current densities with those predicted by the numerical solution using $\alpha = 0.0869$. The theoretical (solid) curves are bounded by dashed curves corresponding to numerical solutions for $D_o = 5.4\times10^{-6}$ $cm^2/sec \pm 10\%$. In view of the uncertainty of the diffusion coefficient for $CuSO_4$, the agreement of the theoretically predicted and interferometrically measured interfacial concentration appears quite satisfactory.

Our agreement with reported diffusion coefficients contrasts with high values, that depended on current density, derived by Tvarusko and Watkins[6] with conventional interpretation of interferograms. For instance, at 23.5 $mA/cm^2$ they found a value of $3.2\times10^{-5}$ $cm^2/s$. We can

entirely account for the observed six-fold derivation in apparent diffusion coefficient as an optical artefact: As can be ssen on Fig. 3, the interference fringe (open circles) indicates an interfacial concentration gradient smaller than the true gradient (closed circles). If the interference fringe is taken as a direct measure of the concentration profile (conventional interpretation), one has to postulate unreasonably high diffusion coefficients in order to account for the imposed current density. We have previously determined different interferometric errors caused by light-deflection:[8] A relative error of -0.83 in concentration gradient at the interface can be estimated from Fig. 10, Ref. 8 for the conditions of this experiment (23.5 $mA/cm^2$, 0.05M concentration difference between bulk and interface). This value is the same as the relative error of the inverse of the reported diffusion coefficient.

Diffusion coefficients presented in O'Brien's interferometric study of $CuSO_4$ diffusion layers[5] also are six times too high initially and decrease with time. The optically derived current densities, based on $D = 4.4\times10^{-6}$ $cm^2/sec$, are only 36-88% of the applied current densities. This anomaly can also be directly attributed to light-deflection effects.

On the other hand, the interferometrically derived concentration profiles presented by Hsueh and Newman[20] are substantially free of light-deflection errors. Their long (40 min) electrolysis times at constant potential resulted in a small interfacial concentration gradient (0.1M $CuSO_4$ $cm^{-1}$) and, consequently, in negligible light-deflection effects.

The derivation of local current densities (or concentration gradients) from interferograms is more difficult than the determination of local concentrations. For all the present experiments, the interferometrically determined current density agreed with the applied current

densities of 5 or 10 mA/cm$^2$ within ±10% (Fig. 6, circles). Conventional interpretation would have resulted in errors up to -68% (Fig. 6, triangles).

The concentration profiles obtained by interferometry can also be analyzed to provide a measure of the cation transference number $t_+$ in 0.1M $CuSO_4$ electrolyte. Equation (12) relates charge passed during constant-current electrolysis to the depletion of $CuSO_4$ within the diffusion layer.

$$i\, t(1 - t_+) = zF \int_0^\infty (C_b - C)\, dx \quad . \tag{12}$$

Cation transference numbers computed by use of Eq. (12) are listed in Table I. The values compare to literature data[17] of 0.36 and 0.40 at C = 0.1M $CuSO_4$ and C = 0, respectively. It can be seen that the conventional interferogram interpretation results in a wide variation of $t_+$ with time and current density.

For short galvanostatic deposition times, concentration profiles obtained for a cathode facing up matched those for one facing down. At times greater than 13 or 18 sec for i = 10 or 5 mA/cm$^2$, respectively, onset of natural convection became apparent by irregular distortions of fringes above the surface.

## CONCLUSIONS

Concentration profiles optically observed near electrodes in the absence of convection agree with those theoretically expected by use of established diffusion coefficients and transference numbers. Thus, we have experimentally corroborated our new techniques[9,19] for deriving one-dimensional concentration distributions from interferograms under consideration of light-deflection and reflection. We can confidently

employ the same optical principles in the analysis of concentration fields near electrodes in the presence of convection, where theoretical solutions are not available.

ACKNOWNLEDGEMENT

This work was conducted under the auspices of the U. S. Energy Research and Development Administration. We also thank the National Aeronautics and Space Administration for a predoctoral traineeship.

## NOMENCLATURE

| | |
|---|---|
| $C$ | electrolyte concentration (M $CuSO_4$) |
| $C_b$ | bulk electrolyte concentration (M $CuSO_4$) |
| $D$ | diffusion coefficient ($cm^2$/sec) |
| $D_o$ | diffusion coefficient at C = 0 ($cm^2$/sec) |
| $F$ | Faraday constant (coul/eq) |
| $i$ | current density ($mA/cm^2$) |
| $N$ | phase change (fringes) |
| $t$ | time after beginning of electrolysis (sec) |
| $t_+$ | cation transference number |
| $x$ | distance from electrode surface (mm) |
| $z$ | cation valence |
| $\alpha$ | constant (Eq. (6)) |
| $\gamma$ | constant (Eq. (7)) |
| $\Delta\phi$ | anode potential minus cathode potential (V) |
| $\theta$ | dimensionless concentration $C/C_b$ |

REFERENCES

1. J. S. Newman, Electrochemical Systems (Prentice-Hall, Inc., Englewood Cliffs, NJ, 1973).
2. R. H. Muller in Advances in Electrochemistry and Electrochemical Engineering, R. H. Muller, ed. (Wiley-Interscience, NY, 1973), Vol. 9, p. 326-353.
3. C. S. Lin, R. W. Moulton and G. L. Putnam, Ind. Eng. Chem. 45, 640 (1953).
4. N. Ibl and R. H. Muller, Z. Elektrochem. 59, 671 (1955).
5. R. N. O'Brien, J. Electrochem. Soc. 113, 389 (1966).
6. A. Tvarusko and L. S. Watkins, Electrochimica Acta 14, 1109 (1969).
7. K. W. Beach, R. H. Muller and C. W. Tobias, J. Opt. Soc. Am. 63, 559 (1973).
8. F. R. McLarnon, R. H. Muller and C. W. Tobias, J. Electrochem. Soc. 122, 59 (1975).
9. F. R. McLarnon, R. H. Muller and C. W. Tobias (submitted to Applied Optics).
10. Surfanalyzer Model 150 Systems, Clevite Corp., Cleveland, Ohio.
11. F. R. McLarnon, Ph. D. Thesis, LBL-3500, Department of Chemical Engineering, University of California, Berkeley, Dec. 1974.
12. K. W. Beach, R. H. Muller and C. W. Tobias, Rev. Sci. Instr. 40, 1248 (1969).
13. K. W. Beach, Ph. D. Thesis, UCRL-20324, Department of Chemical Engineering, University of California, Berkeley (University Microfilms, Ann Arbor, Mich., order No. 72-13269).

14. L. Lapidus, Digital Computation for Chemical Engineers (McGraw-Hill, N. Y., 1962), p. 162.

15. Ibid, p. 254-255.

16. W. G. Eversole, H. M. Kindsvater and J. D. Peterson, J. Phys. Chem. 46, 370 (1942).

17. J. J. Fritz and C. R. Fuget, J. Phys. Chem. 62, 303 (1958).

18. H. J. S. Sand, Phil. Mag. 1[6], 45 (1901).

19. F. R. McLarnon, R. H. Muller and C. W. Tobias (submitted to J. Opt. Soc. Am.).

20. L. Hsueh and J. Newman, Electrochimica Acta 16, 479 (1971).

Table I. Cation transference numbers derived from interferometrically determined concentration profiles.

| i ($mA/cm^2$) | t(s) | Present interferogram Interpretation $t_+$ | Conventional interferogram Interpretation $t_+$ |
|---|---|---|---|
| 5 | 10 | 0.377 | 0.212 |
| 5 | 30 | 0.388 | 0.062 |
| 5 | 50 | 0.415 | 0.070 |
| 10 | 10 | 0.414 | 0.439 |
| 10 | 20 | 0.448 | 0.357 |
| 10 | 30 | 0.429 | 0.289 |
| 10 | 40 | 0.431 | 0.261 |

## FIGURE CAPTIONS

Fig. 1. Interferometer and electrochemical cell cross section.

——— Light path

- - - - Off-axis rays demonstrating point-to-point relationship between plane of focus and film plane

A Copper anode

C Copper cathode

E 0.1 M $CuSO_4$ electrolyte

F Film plane

G Glass sidewalls

L Lens. The test lens (focal length 87 mm) is 115 mm from the center of the cell. The focal length of the reference lens in 81 mm.

M Mirror

S Light source (HeNe laser)

U Beam uniter

d 12.7 mm

h 25.4 mm

w 10.0 mm

Fig. 2. $CuSO_4$ diffusion coefficient.

——— Smoothed data of Eversole et al.,[16] corrected to 20°C

— — — — Linear approximation, $D = (5.41 - 4.70\ C) \times 10^{-6}$

. — . Linear approximation, $D = (5.75 - 8.11\ C) \times 10^{-6}$

Fig. 3. Interferogram interpretation.

ordinate: distance from electrode surface (mm)

abscissa: electrolyte concentration (M $CuSO_4$) or interferometric phase change (fringes)

o o o o experimental interferogram, i = 10.0 $mA/cm^2$, $C_b$ = 0.1 M $CuSO_4$, t = 30 sec, cathode faces down.

- - - - concentration profile derived from experimental interferogram

——— computed interferogram associated with derived concentration profile

• • • • theoretical concentration profile computed by numerical techniques for $\alpha = 0.0869$

A apparent interfacial location on the experimental interferogram

B apparent interfacial location on the computed interferogram

Fig. 4. Transient interfacial concentrations. i = 10.0 $mA/cm^2$.

ordinate: interfacial concentration $C_s$ (M $CuSO_4$) or cell voltage $\Delta\phi$ (volts)

abscissa: time after beginning of electrolysis (sec)

— — — — numerical solution for $\alpha = 0$ (corresponds to the Sand equation) $t_+ = 0.364$, $D = 4.94\times10^{-6}$

——— numerical solution for $\alpha = 0.0869$, $D_o = 5.41\times10^{-6}$ cm/s, $\gamma = 0.0648$

— · — · numerical solution for $\alpha = 0.141$, $D_o = 5.75\ 10^{-6}$ $cm^2/s$, $\gamma = 0.0648$

• interferometrically determined interfacial concentrations

Fig. 5. Transient interfacial concentrations, i = 5.0 and 10.0 mA/cm$^2$.

——— numerical solution for $\alpha = 0.0869$, $D_o = 5.41\times10^{-6}$ cm$^2$/sec, $\gamma = 0.0648$

– – – – ±10% uncertainty in diffusion coefficient $D_o$

• interferometrically determined interfacial concentrations

Fig. 6. Derived current densities.

△ ▲ conventional analysis of the experimental interferograms

○ ● analysis considering light-deflection and edge reflection

-▲-●- applied current 5.0 mA/cm$^2$ (shaded area ±10%)

-△-○- applied current 10 mA/cm$^2$ (shaded area ±10%)

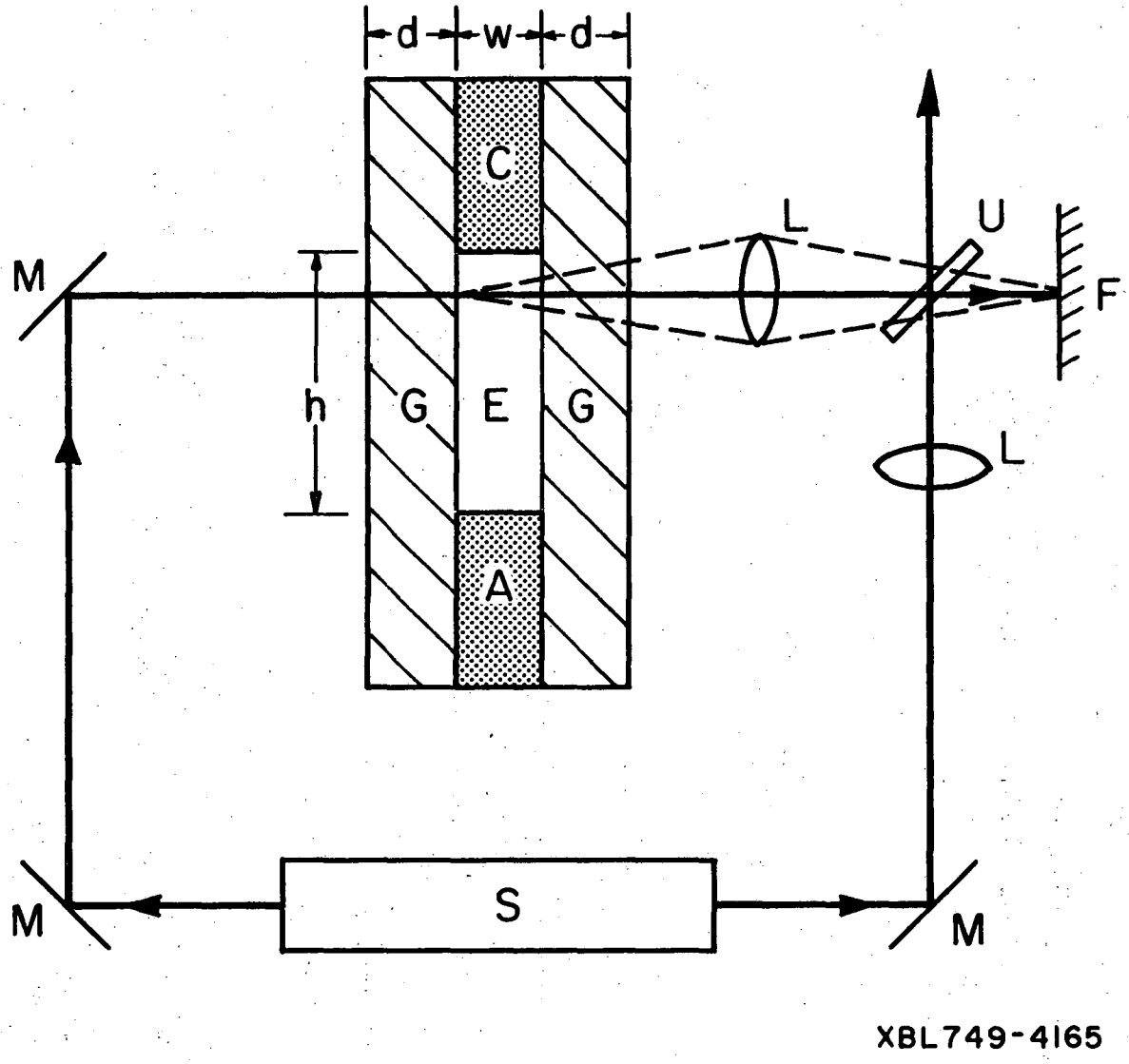


Fig. 1

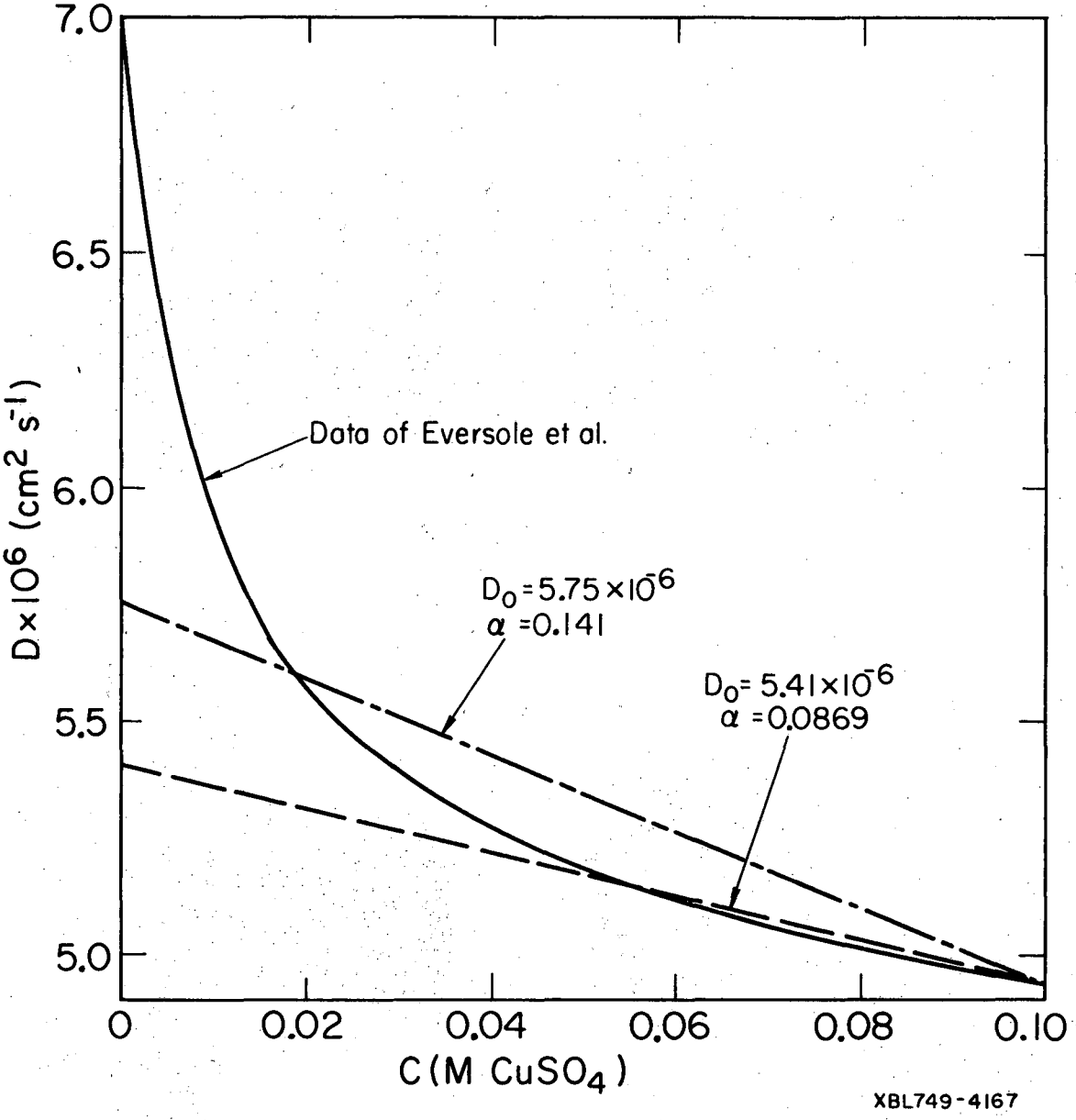


Fig. 2

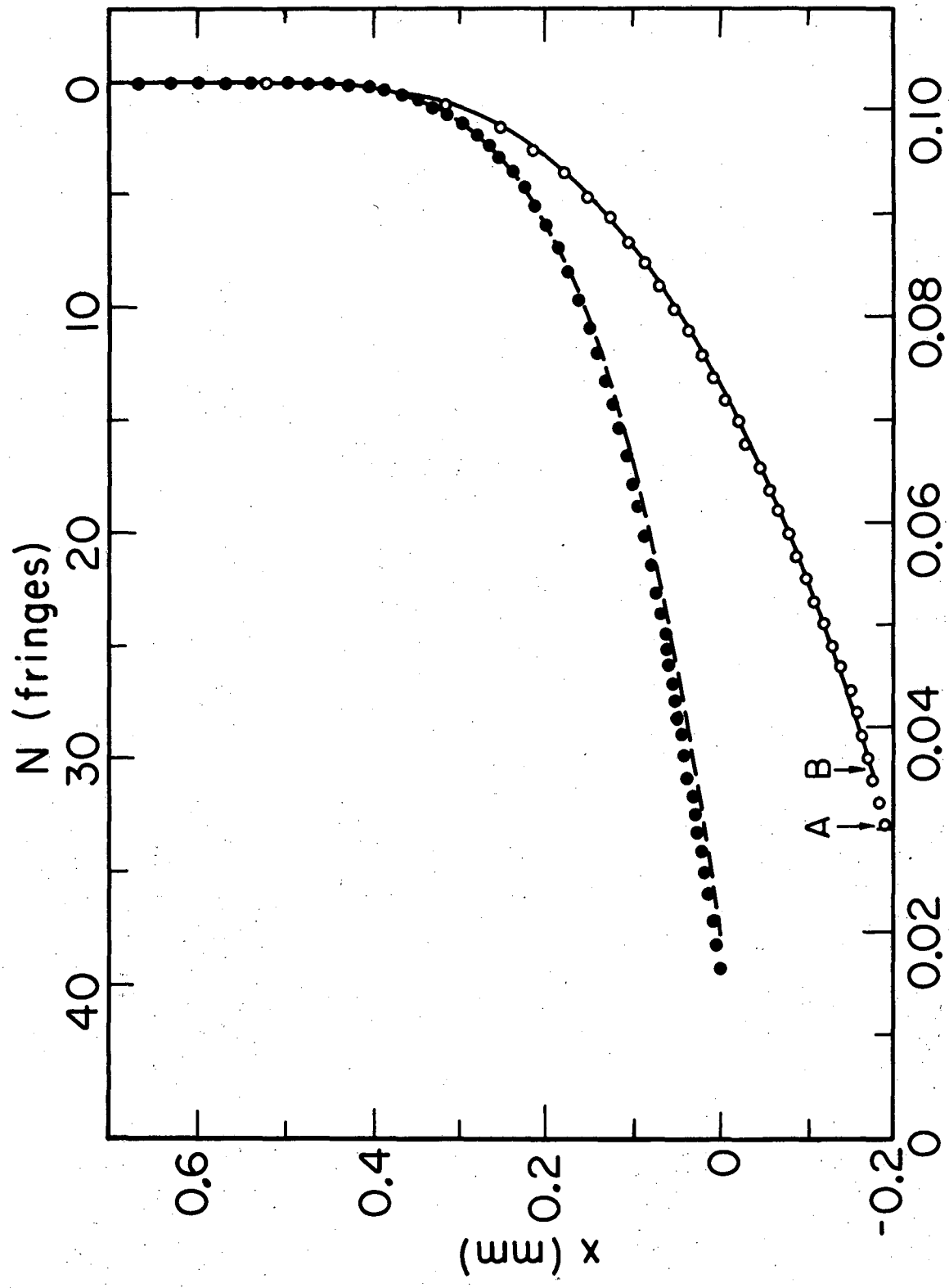


XBL7411-4580

Fig. 3

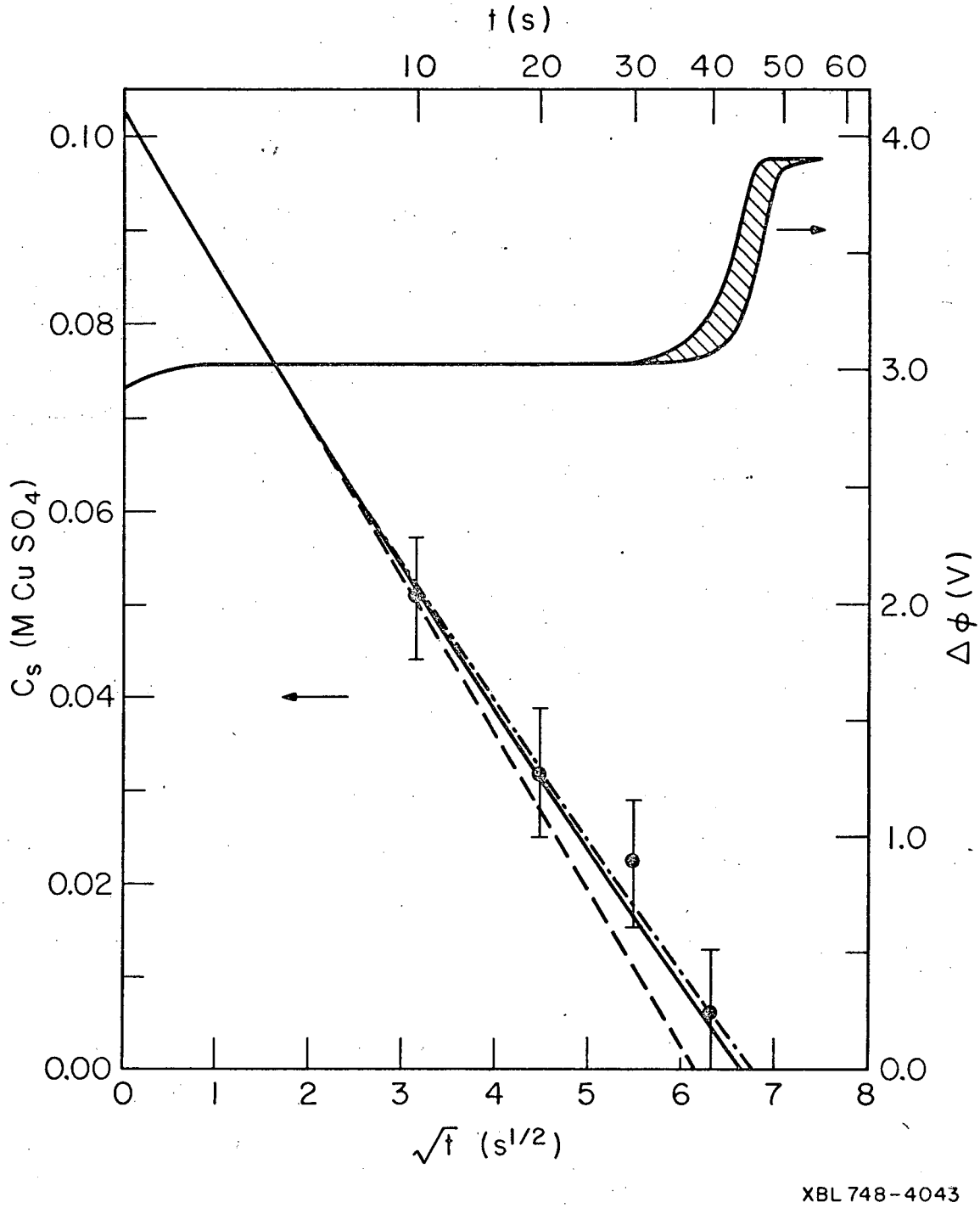


Fig. 4

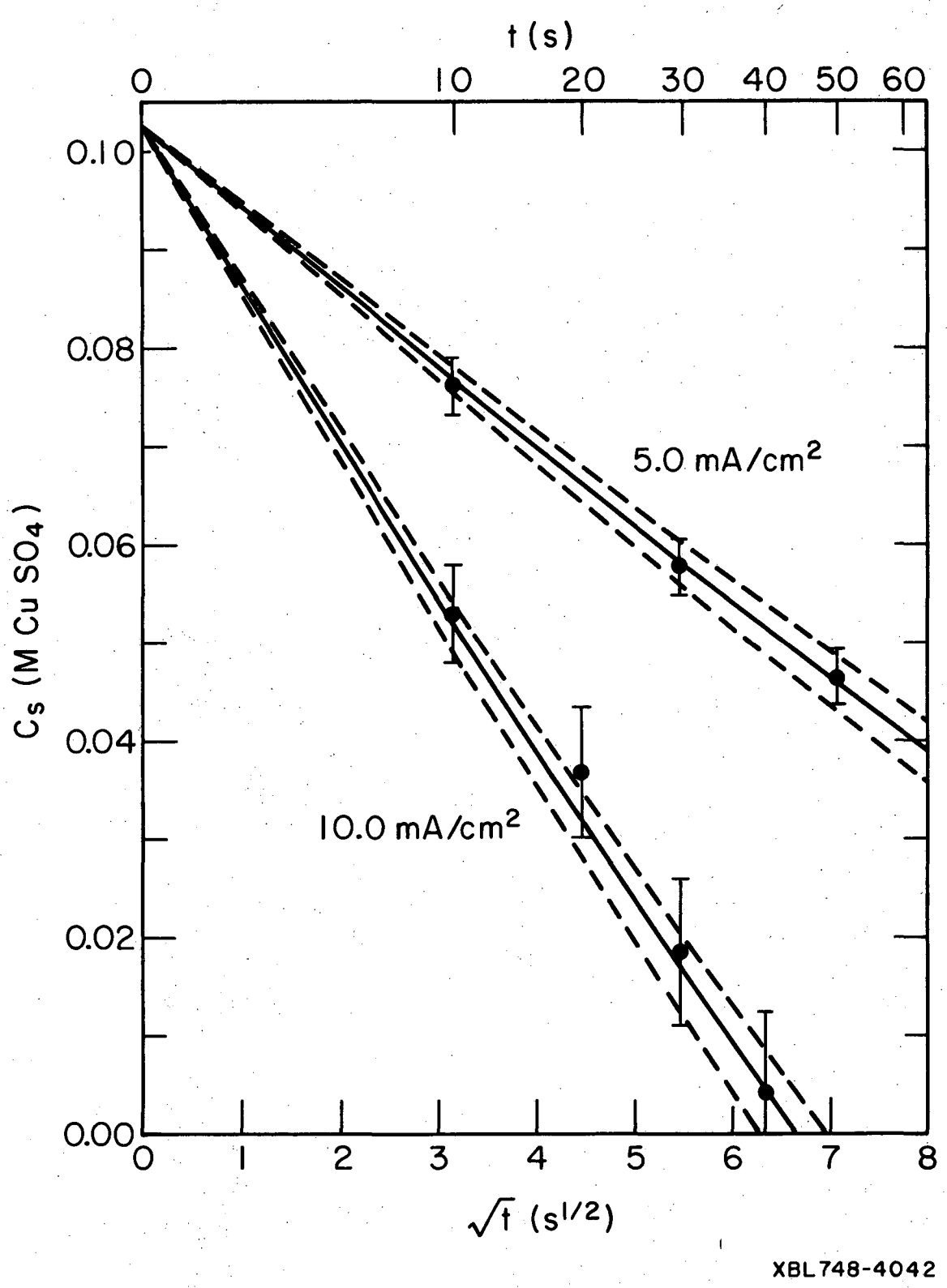
t (s)
0
10
20
30
40
50
60
0.10
0.08
0.06
0.04
0.02
0.00
$C_s$ (M Cu $SO_4$)
5.0 mA/cm$^2$
10.0 mA/cm$^2$
0
1
2
3
4
5
6
7
8
$\sqrt{t}$ ($s^{1/2}$)
XBL748-4042

Fig. 5

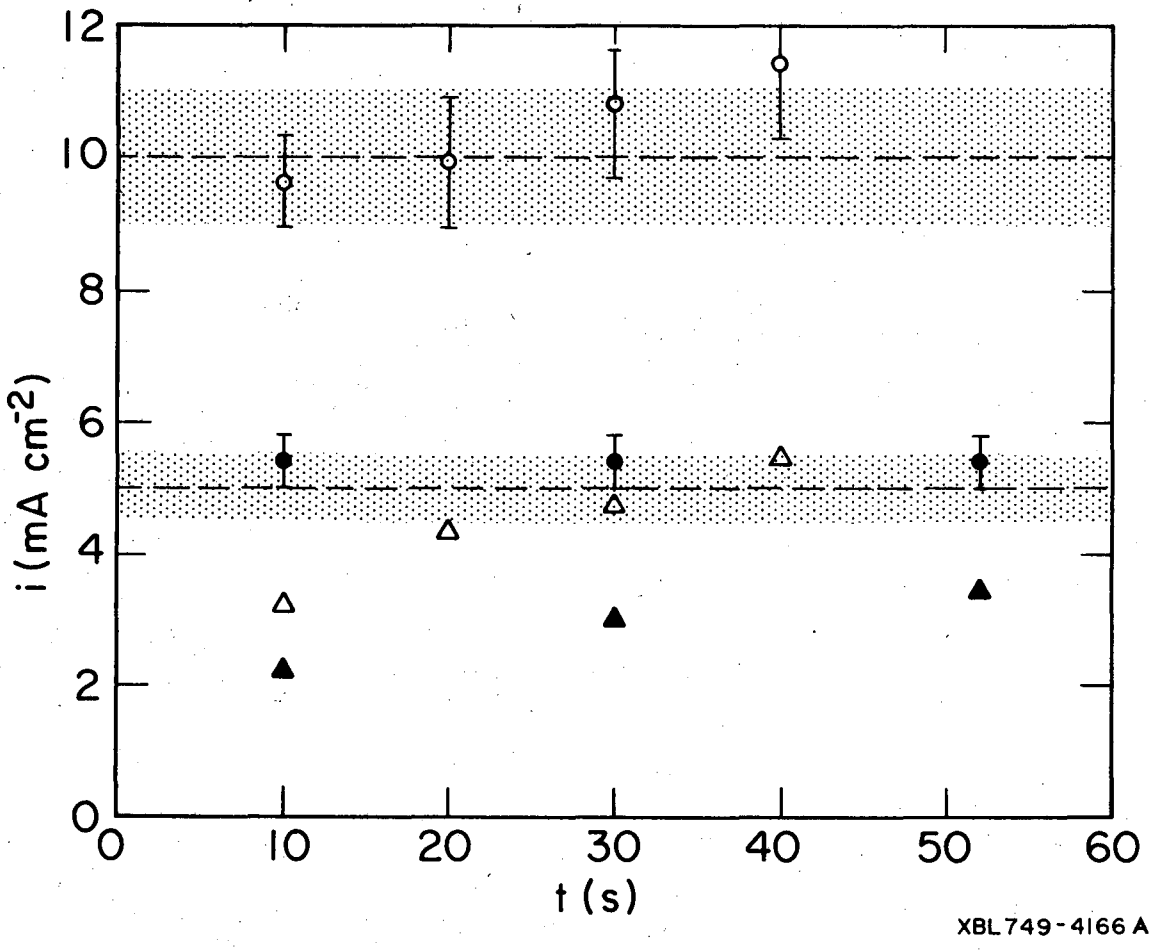


Fig. 6

*TECHNICAL INFORMATION DIVISION*
*LAWRENCE BERKELEY LABORATORY*
*UNIVERSITY OF CALIFORNIA*
*BERKELEY, CALIFORNIA 94720*